Exploring nonlinear subgrid-scale models and new characteristic length scales for large-eddy simulation

By M. H. Silvis†, F. X. Trias‡, M. Abkar, H. J. Bae, A. Lozano-Durán AND R. W. C. P. Verstappen†

We study subgrid-scale modeling for large-eddy simulation (LES) of anisotropic turbulent flows on anisotropic grids. In particular, we show how the addition of a velocity-gradient-based nonlinear model term to an eddy viscosity model provides a better representation of energy transfer. This is shown to lead to improved predictions of rotating and nonrotating homogeneous isotropic turbulence. Our research further focuses on calculation of the subgrid characteristic length, a key element for any eddy viscosity model. In the current work, we propose a new formulation of this quantity based on a Taylor series expansion of the subgrid stress tensor in the computational space. Numerical tests of decaying homogeneous isotropic turbulence and a plane-channel flow illustrate the robustness of this flow-dependent characteristic length scale with respect to mesh anisotropy.

1. Introduction

Most practical turbulent flows cannot be computed directly from the Navier-Stokes equations, because not enough resolution is available to resolve all relevant scales of motion. We therefore turn to LES to predict the large-scale behavior of incompressible turbulent flows. In LES, the large scales of motions in a flow are explicitly computed, whereas the effects of small-scale motions are modeled. Since the advent of computational fluid dynamics, many subgrid-scale models have been proposed and successfully applied to a wide range of flows, cf., for instance, Sagaut (2006).

In the current work, we focus on subgrid-scale modeling for LES of anisotropic flows on anisotropic grids. On the one hand, we look to go beyond the purely dissipative description of turbulent flows that is provided by eddy viscosity models. To that end, we consider model terms that are nonlinear in the velocity gradient, which can capture convective transport of energy among large scales of motion. This will likely lead to an improved prediction of flows in which the subgrid-scale stress anisotropy plays an important role, such as in rotating flows (Marstorp *et al.* 2009). On the other hand, we aim to find a proper definition of the subgrid characteristic length scale that minimizes the dependence of simulation results on grid anisotropy. This is particularly important for simulations on highly anisotropic or stretched grids, for which the smallest grid spacing may start dominating the characteristic length scale that is commonly used. In this work a new flow-dependent characteristic length scale is proposed.

We explore the behavior of subgrid-scale models of eddy viscosity and nonlinear form in

† University of Groningen, The Netherlands
‡ Technical University of Catalonia, Spain

simulations of rotating homogeneous isotropic turbulence and spanwise-rotating plane-channel flow. Furthermore, the new flow-dependent subgrid characteristic length scale is studied in simulations of nonrotating homogeneous isotropic turbulence and plane-channel flow. A comparison is made with other characteristic length scales.

The outline of this paper is as follows. The basic equations of LES are introduced in Section 2, along with subgrid-scale models that are nonlinear in the velocity gradient. A new flow-dependent subgrid characteristic length scale is also proposed. Section 3 discusses the particular numerical test cases considered in this work, as well as results of LES and direct numerical simulations (DNS). Finally, Section 4 provides the study's conclusions and an outlook for future research.

2. Background

2.1. *Large-eddy simulation*

In LES, usually a filtering or coarse-graining operation is employed to distinguish between large and small scales of motion in flows. This operation is denoted by an overbar in what follows. The evolution of incompressible, rotating large-scale velocity fields can be described by the filtered Navier-Stokes equations in a rotating frame, supplemented by the incompressibility constraint (Sagaut 2006; Grundestam *et al.* 2008),

$$\frac{\partial \bar{u}_i}{\partial t} + \bar{u}_j \frac{\partial \bar{u}_i}{\partial x_j} = -\frac{1}{\rho}\frac{\partial \bar{p}}{\partial x_i} + \nu \frac{\partial^2 \bar{u}_i}{\partial x_j \partial x_j} + 2\epsilon_{ijk}\bar{u}_j\Omega_k - \frac{\partial}{\partial x_j}\tau_{ij}, \qquad \frac{\partial \bar{u}_i}{\partial x_i} = 0. \tag{2.1}$$

Here, $\bar{u}_i$ represents the x_i-component of the filtered velocity field and $\bar{p}$ indicates the filtered pressure. Alternatively, the coordinates may be written x, y and z. The density and kinematic viscosity are denoted by ρ and ν, and are taken constant. The rotation vector, appearing in the Coriolis force, is represented by Ω_k. Einstein's summation convention is assumed for repeated indices. The turbulent, or subgrid-scale, stresses, $\tau_{ij} = \overline{u_i u}_j - \bar{u}_i \bar{u}_j$, represent the interactions between large and small scales of motion. As they are not solely expressed in terms of the filtered velocity field, they have to be modeled.

2.2. *Nonlinear subgrid-scale models*

We assume that the subgrid-scale stresses can be fully characterized by the local large-scale velocity gradient,

$$G_{ij} = \frac{\partial \bar{u}_i}{\partial x_j}, \tag{2.2}$$

and consider subgrid-scale models of the following nonlinear form (Pope 1975; Lund & Novikov 1992),

$$\tau^{\mathrm{mod}} - \frac{1}{3}\,\mathrm{tr}(\tau^{\mathrm{mod}})I = -2\nu_e S + \mu_e(S\Omega - \Omega S). \tag{2.3}$$

Here, the filtered rate-of-strain and rate-of-rotation tensors are given by

$$S_{ij} = \frac{1}{2}\left(\frac{\partial \bar{u}_i}{\partial x_j} + \frac{\partial \bar{u}_j}{\partial x_i}\right), \qquad \Omega_{ij} = \frac{1}{2}\left(\frac{\partial \bar{u}_i}{\partial x_j} - \frac{\partial \bar{u}_j}{\partial x_i}\right). \tag{2.4}$$

The model coefficients, ν_e and μ_e, are usually defined as a product of three factors: a dimensionless constant; a (squared) length scale, such as the LES filter length or characteristic length scale, δ; and a function with units of inverse time, that depends on the local large-scale velocity gradient via the tensor invariants

$$I_1 = \mathrm{tr}(S^2), \quad I_2 = \mathrm{tr}(\Omega^2), \quad I_3 = \mathrm{tr}(S^3), \quad I_4 = \mathrm{tr}(S\Omega^2), \quad I_5 = \mathrm{tr}(S^2\Omega^2). \tag{2.5}$$

The first term on the right-hand side of Eq. (2.3), the usual eddy viscosity term, is used to parametrize dissipative processes in turbulent flows. The second term, that is nonlinear in the velocity gradient, is added because it is perpendicular to the rate-of-strain tensor. Therefore, it does not directly contribute to the subgrid dissipation and it has to represent energy transport. This may be important to better capture the behavior of scales of motion of the order of the subgrid characteristic length scale. Marstorp *et al.* (2009) show that addition of a nonlinear term of the form $\mu_e(S\Omega - \Omega S)$ to an eddy viscosity model can significantly improve prediction of the Reynolds stresses in rotating and nonrotating turbulent channel flows. Follow-up research by Rasam *et al.* (2011) and Montecchia *et al.* (2015) indicates that such a model also performs well at coarse resolutions. As the nonlinear model term contains the rate-of-rotation tensor, it has "a particular potential for [the simulation of] rotating flows" (Marstorp *et al.* 2009). The particular choice of subgrid-scale models in this study is detailed in Section 3.

2.3. *A new subgrid characteristic length scale*

As discussed in Section 2.2, subgrid-scale models that depend on the local velocity gradient (usually) require specification of what we call the subgrid characteristic length scale, δ. This length scale is generally associated with the local grid size. That is, for isotropic grids, δ is assumed to be equal to the mesh size, $\delta = \Delta x = \Delta y = \Delta z$. However, for anisotropic or unstructured grids, a consensus has not yet been reached.

Owing to its simplicity, the most widely used approach is that proposed by Deardorff (1970), based on the cube root of the cell volume. For a Cartesian grid it reads

$$\delta_{\text{vol}} = (\Delta x \Delta y \Delta z)^{1/3}. \tag{2.6}$$

Extensions of this approach for anisotropic grids were proposed by, for instance, Scotti *et al.* (1993). Alternative definitions of δ include the maximum of the cell sizes,

$$\delta_{\max} = \max(\Delta x, \Delta y, \Delta z), \tag{2.7}$$

which was originally proposed in the first presentation of Detached-Eddy Simulation (DES) by Spalart *et al.* (1997) as a safer and robust definition of δ.

More recent definitions of δ are also found in the context of DES. For example, Chauvet *et al.* (2007) introduced the concept of sensitizing the characteristic length scale to the orientation of the vorticity vector, $\omega_i = \epsilon_{ijk}\partial_j u_k$,

$$\delta_\omega = \sqrt{(\omega_x^2 \Delta y \Delta z + \omega_y^2 \Delta x \Delta z + \omega_z^2 \Delta x \Delta y)/|\omega|^2}. \tag{2.8}$$

This definition detects the alignment of the vorticity vector, ω_i, whose magnitude is written $|\omega| = \sqrt{\omega_i \omega_i}$, with an axis. For example, if $\omega_i = \delta_{i3}\omega_z$ we obtain $\delta_\omega = \sqrt{\Delta x \Delta y}$. This approach was motivated by the fact that $\delta_{\max}$ results in an excessive generation of eddy viscosity in the initial region of shear layers typically resolved on highly anisotropic grids. However, like Deardorff's length scale given in Eq. (2.6), δ_ω may still involve the smallest of the grid spacings. This may lead to very low values of eddy viscosity.

The concept of a flow-dependent length scale is very appealing. As flows can be characterized using the resolved velocity field gradient, Eq. (2.2), it seems logical to employ this tensor quantity to create a flow-dependent definition of δ. Both the subgrid characteristic length, δ, and the velocity gradient tensor, G, appear in a natural way when we consider the leading-order Taylor series expansion of the subgrid-scale stress tensor in the filter

length, δ,

$$\tau = \frac{\delta^2}{12} GG^T + \mathcal{O}(\delta^4). \tag{2.9}$$

For anisotropic filter lengths, the Taylor expansion of the subgrid stress tensor gives

$$\tau = \frac{1}{12} G_\delta G_\delta^T + \mathcal{O}(\delta^4), \tag{2.10}$$

where $G_\delta \equiv G\Delta$, and the local mesh geometry for a Cartesian grid is contained in the second-order diagonal tensor

$$\Delta \equiv \mathrm{diag}(\Delta x, \Delta y, \Delta z). \tag{2.11}$$

Performing a least-squares minimization of the difference between the leading-order terms of Eqs. (2.9)-(2.10), i.e., $(\delta^2/12)GG^T \approx (1/12)G_\delta G_\delta^T$, we obtain

$$\delta_{\mathrm{lsq}} = \sqrt{\frac{G_\delta G_\delta^T : GG^T}{GG^T : GG^T}}. \tag{2.12}$$

Here, the double dot represents the Frobenius inner product of two tensors, which is akin to the dot product for vectors. The length scale δ_{lsq} is defined locally and is well-bounded, $\delta_{\min} \leq \delta_{\mathrm{lsq}} \leq \delta_{\max}$, where $\delta_{\max}$ is given in Eq. (2.7) and $\delta_{\min}$ is defined analogously. Moreover, it is obviously sensitive to flow orientation. In this regard, for purely rotating flows, i.e., $S = 0$ and $G = \Omega$, δ_{lsq} reduces to

$$\delta_{\mathrm{lsq}} = \sqrt{\frac{\omega_x^2(\Delta y^2 + \Delta z^2) + \omega_y^2(\Delta x^2 + \Delta z^2) + \omega_z^2(\Delta x^2 + \Delta y^2)}{2|\omega|^2}}, \tag{2.13}$$

which resembles the definition of δ_ω given in Eq. (2.8). Note that, for $\omega_i = \delta_{i3}\omega_z$, δ_{lsq} is $\mathcal{O}(\max\{\Delta x, \Delta y\})$ instead of being equal to $\sqrt{\Delta x \Delta y}$. Therefore, the definition δ_{lsq} also avoids a strong effect of the smallest grid spacing.

3. Numerical results

In the current project, we performed DNS and LES of rotating and nonrotating decaying homogeneous isotropic turbulence and turbulent plane-channel flow. A detailed description of these simulations and their results is provided below. All simulations were performed using incompressible Navier-Stokes solvers that employ kinetic-energy-conserving spatial discretizations of finite-difference or finite-volume type (Verstappen & Veldman 2003).

3.1. *Exploring subgrid-scale models*

3.1.1. *Rotating homogeneous isotropic turbulence*

We first consider simulations of decaying homogeneous isotropic turbulence, set up according to the description provided by Rozema *et al.* (2015). The addition of rotation is characterized by the bulk rotation number $\mathrm{Ro} = 2\Omega L/u_{\mathrm{ref}}$. Here, L represents the size of the box of turbulence considered, $\Omega = \Omega_3$ is the rotation rate about the z-axis and u_{ref} is a reference velocity corresponding to the initial kinetic energy content of the flow. Time is nondimensionalized according to $0.0024L/u_{\mathrm{ref}}$ (Rozema *et al.* 2015). The direct numerical simulations were performed on a uniform, isotropic 512^3 grid, whereas a 64^3 grid was used for the LES. In the latter, we used a new implementation of the minimum-dissipation model of Rozema *et al.* (2015), with and without the nonlinear model term

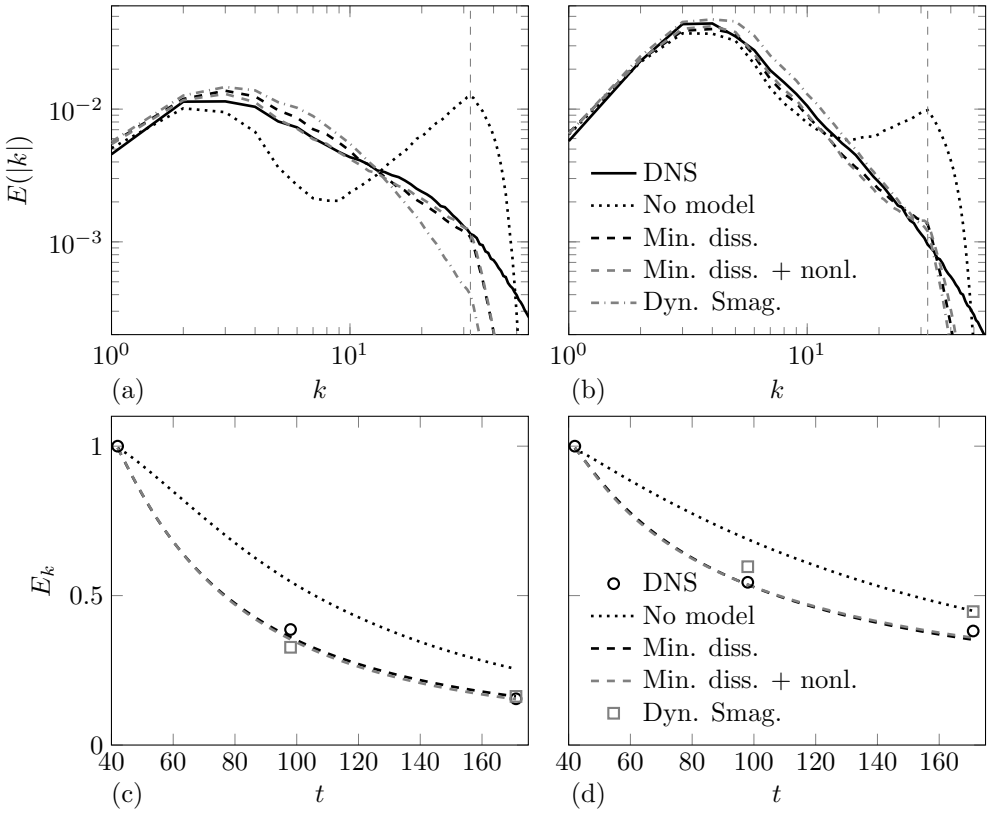

FIGURE 1. Three-dimensional kinetic energy spectra as a function of computational wavenumber at nondimensional time $t = 171$ for (a) Ro = 0 and (b) Ro = 100, and decay of the normalized total resolved kinetic energy for (c) Ro = 0 and (d) Ro = 100. Results were obtained from a direct numerical simulation and from LES without a model, with the minimum-dissipation model (with and without addition of a nonlinear term) and with the dynamic Smagorinsky model. The dashed vertical line in the top figures represents the grid point-to-point oscillation.

of Eq. (2.3). In this preliminary study, the coefficient of the nonlinear model is taken independent of the flow field, $\mu_e = C_\mu \delta^2$, where C_μ is a constant and the characteristic length scale is straightforwardly defined as $\delta = \Delta x = \Delta y = \Delta z$. Also the dynamic Smagorinsky model (Germano *et al.* 1991) was used.

Figure 1 shows three-dimensional kinetic energy spectra and the decay of the normalized total resolved kinetic energy for rotation numbers Ro = 0 (no rotation) and Ro = 100 (significant rotation). As expected, the Coriolis force makes the transport of energy to larger scales of motion grow. As a consequence, the dissipation rate of kinetic energy decreases. Without rotation (Ro = 0), the minimum-dissipation model overpredicts the large-scale and underpredicts the small-scale kinetic energy. Addition of the nonlinear term ($C_\mu = -0.09$) can correct for this by increasing the forward scatter of energy. For the case with rotation (Ro = 100), the minimum-dissipation model underpredicts the kinetic energy for both large and intermediate length scales. The nonlinear model term can also transport energy to larger scales (backscatter). Although this effect is small for the higher rotation numbers, it occurs for $0 \leq C_\mu \leq 0.5$ and Ro < 100 (not shown). The nonlinear term does not have a large effect on the total resolved kinetic energy, confirm-

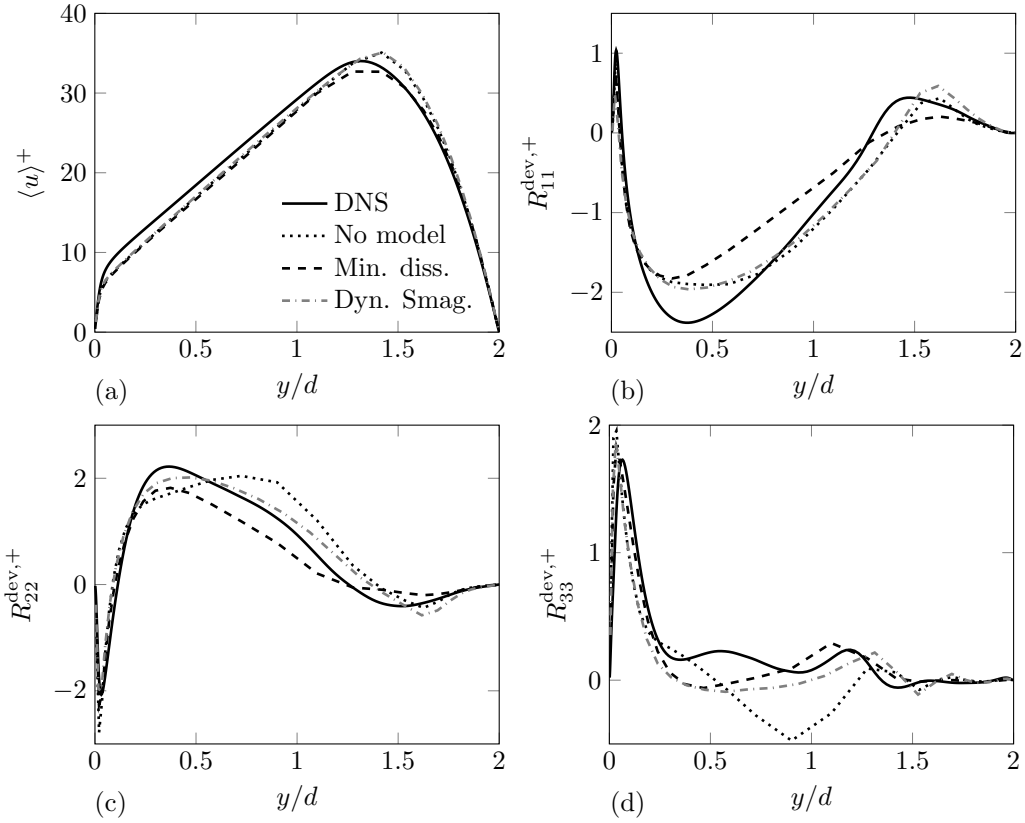

FIGURE 2. Mean velocity profile (a) and deviatoric diagonal Reynolds stresses in the streamwise (b), wall-normal (c) and spanwise (d) directions at rotation number $\mathrm{Ro}^+ = 22$ and $\mathrm{Re}_\tau = 180$. Results were obtained from a direct numerical simulation and from LES without a model, with the minimum-dissipation model and with the dynamic Smagorinsky model.

ing that it describes energy transfer rather than dissipation. The dynamic Smagorinsky model appears to consistently overpredict the large-scale kinetic energy content. Without rotation ($\mathrm{Ro} = 0$), the predicted small-scale kinetic energy is too small with respect to the direct numerical simulation. This can be understood from the use of explicit filtering in determining the model constant, which damps motions close to the cutoff (Rozema *et al.* 2015). For the case with rotation ($\mathrm{Ro} = 100$), however, the dynamic Smagorinsky model predicts the small-scale kinetic energy content accurately, perhaps because the flow is essentially becoming two-dimensional under rotation.

3.1.2. *Rotating plane-channel flow*

We also performed simulations of spanwise-rotating plane-channel flow. These simulations were set up according to the work of Grundestam *et al.* (2008) and can be characterized by the friction Reynolds number $\mathrm{Re}_\tau = u_\tau d/\nu$ (where u_τ is the friction velocity derived from the wall shear stress and d is the channel half-width) and the rotation number $\mathrm{Ro}^+ = 2\Omega d/u_\tau$ (where $\Omega = \Omega_3$ represents the rotation rate about the spanwise axis). The flow domain was taken to be of size $4\pi d \times 2d \times 2\pi d$ for simulations at $\mathrm{Re}_\tau = 180$. Direct numerical and LES were, respectively, performed on $256 \times 192 \times 192$ and $64 \times 32 \times 64$ grids that were stretched in the wall-normal directions, but were uni-

form in wall-parallel planes. We considered the effects of the minimum-dissipation and dynamic Smagorinsky models. Study of the addition of nonlinear model terms will be deferred to future work, because we first need to investigate the effects of different length scale definitions on stretched grids (refer to Section 3.2).

Figure 2 shows simulation results for the mean velocity profile and deviatoric diagonal parts of the Reynolds stresses, $R_{ij} = \langle u_i u_j \rangle - \langle u_i \rangle \langle u_j \rangle$, where $\langle \cdot \rangle$ represents a time average. We compare the deviatoric Reynolds stresses, because the subgrid-scale models we consider are traceless, i.e., they do not include a model for the subgrid-scale kinetic energy. Although Re_τ is relatively small (i.e., 180), results obtained from direct numerical simulations and LES without a model are quite distinct. This indicates that subgrid-scale modeling is indeed necessary at the current resolution.

Figure 2(a) shows that all simulation results predict well the typical slope of Ro^+ that is due to laminarization of the flow on the stable side ($y/d = 2$) of the rotating channel. Only the minimum-dissipation model provides a good prediction of the location of the peak of the mean velocity profile. The dynamic Smagorinsky model seems to follow closely the no-model mean velocity profile, also reflected in the streamwise Reynolds stresses. The Reynolds stress profiles show that results obtained using the minimum-dissipation and dynamic Smagorinsky models qualitatively follow the DNS results, but quantitative improvements are clearly necessary. Note, however, that the average contribution of the model to the Reynolds stresses was not taken into account. Once we compensate for this, it might be possible to obtain an improved match between LES and direct numerical simulation results (Winckelmans *et al.* 2002).

3.2. *Exploring subgrid characteristic length scales*

3.2.1. *Homogeneous isotropic turbulence*

The numerical simulation of decaying isotropic turbulence was chosen as a first case to test the novel length scale, δ_{lsq}, proposed in Eq. (2.12). The configuration corresponds to the classical experiment of Comte-Bellot & Corrsin (1971). Large-eddy simulation results have been obtained using the Smagorinsky model, for a set of (artificially) stretched meshes, namely $32 \times 32 \times N_z$, where $N_z = \{32, 64, 128, 256, 512, 1024, 2048\}$. Results are displayed in Figure 3. As expected, for increasing values of N_z the results obtained using the classical definition of Deardorff, given in Eq. (2.6), diverge. This is because the value of δ tends to vanish and, therefore, the subgrid-scale models switch off. Such is not the case for the definition of δ proposed in this work. On the contrary, the results rapidly converge for increasing values of N_z. Therefore, the newly proposed length scale, δ_{lsq}, seems to minimize the effect of mesh anisotropies on the performance of subgrid-scale models.

3.2.2. *Plane-channel flow*

To test the performance of the proposed definition of δ_{lsq} in the presence of walls, simulations of a turbulent channel flow have also been considered. In this case, the code is based on a fourth-order symmetry-preserving finite volume discretization (Verstappen & Veldman 2003) of the incompressible Navier-Stokes equations on structured staggered grids. For the spatial discretization of the eddy viscosity models, the novel approach proposed by Trias *et al.* (2013) has been used in conjunction with the S3PQ model (Trias *et al.* 2015). Results obtained for a set of (artificially) stretched grids are displayed in Figure 4. The starting point corresponds to a 32^3 mesh which suffices to obtain a good agreement with the DNS data (Trias *et al.* 2015). Two additional meshes (with $N_z = 128$

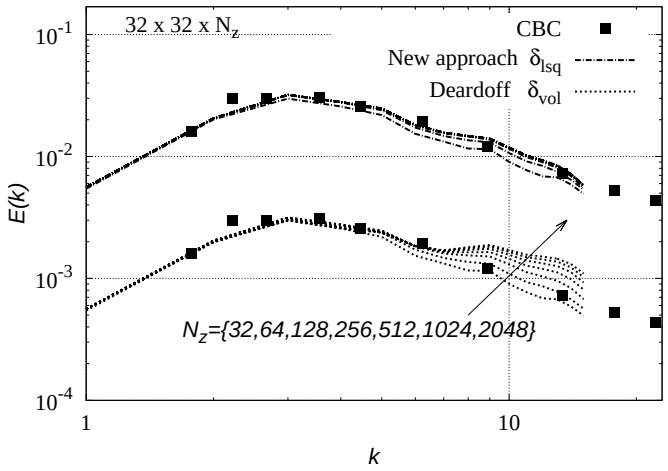

FIGURE 3. Three-dimensional kinetic energy spectra as a function of computational wavenumber, for decaying isotropic turbulence corresponding to the experiment of Comte-Bellot & Corrsin (1971). Large-eddy simulation results have been obtained with a set of anisotropic meshes using the Smagorinsky model. Results obtained with the novel length scale, δ_{lsq}, proposed in Eq. (2.12) (top) are compared with the classical definition of Eq. (2.6) proposed by Deardorff (bottom). For clarity, the latter results are shifted one decade down.

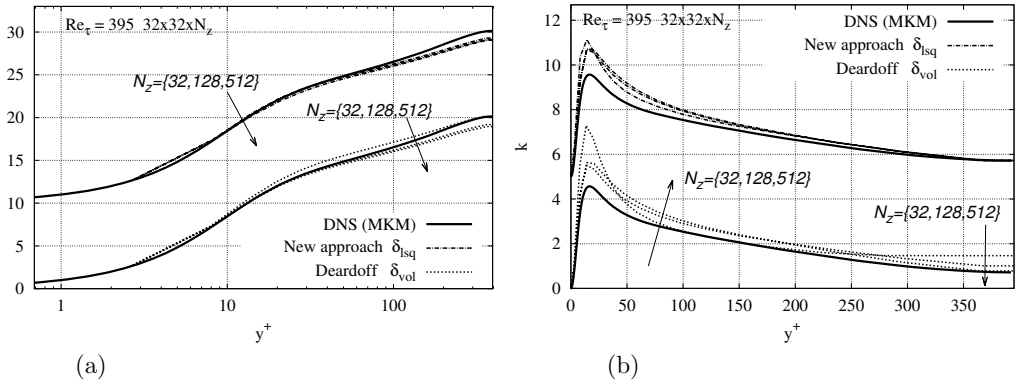

FIGURE 4. Results for a turbulent channel flow at $\mathrm{Re}_\tau = 395$ obtained with a set of anisotropic meshes using the S3PQ model (Trias *et al.* 2015). Solid lines corresponds to the direct numerical simulation of Moser *et al.* (1999). Results obtained with the novel length scale, δ_{lsq}, proposed in Eq. (2.12) are compared with the classical definition proposed by Deardorff given in Eq. (2.6). For clarity, the former results are shifted upward. (a) Mean streamwise velocity, $\langle u \rangle$; (b) turbulent kinetic energy, k.

and $N_z = 512$) have been employed to investigate the effect of δ. Refinement in the spanwise direction was chosen because this was expected to have a smaller influence on numerical results than refinement in, for example, the wall-normal direction. As such, differences in numerical results can be attributed to a different choice of length scale.

Again, the results obtained with the new definition of δ are much more robust to mesh anisotropies. No changes are observed in the mean velocity profile when the newly proposed length scale is employed, whereas significant changes are observed for Deardorff's classical definition. Similar behavior is observed for the turbulent kinetic energy,

especially in the bulk region, where results obtained with the new definition are almost independent of the value of N_z.

4. Conclusions

We studied subgrid-scale modeling for LES of anisotropic turbulent flows on anisotropic grids. We aimed to go beyond the purely dissipative description of turbulent flows that is provided by eddy viscosity models. We therefore explored adding a nonlinear model term to the minimum-dissipation eddy viscosity model of Rozema *et al.* (2015). DNS and LES of rotating homogeneous isotropic turbulence showed that this nonlinear model term (with constant coefficient) can lead to enhanced forward scatter of energy. It was also shown that the nonlinear term can capture transfer of energy from small to large scales of motion (backscatter), confirming the potential of such a term to describe energy transport in turbulent flows. The nonlinear model term can, to a certain extent, correct the prediction of kinetic energy spectra obtained using the minimum-dissipation model. The dynamic Smagorinksy model, used as reference, appeared to overpredict the kinetic energy of large-scale motions in nonrotating and rotating homogeneous isotropic turbulence. While underpredicting the small-scale kinetic energy in the nonrotating case, the dynamic Smagorinksy model predicted this quantity well in homogeneous isotropic turbulence with rotation. Simulations of spanwise-rotating plane-channel flow also showed that, despite the low Reynolds number of $\mathrm{Re}_\tau = 180$, DNS and LES without a model are clearly distinguishable. This underlines the need for subgrid-scale modeling in such flows. Although the mean velocity profile and Reynolds stresses obtained from LES using the minimum-dissipation model and the dynamic Smagorinsky model showed qualitative agreement with results from direct numerical simulations, quantitative improvements are necessary, particularly, for the Reynolds stresses. Rotating flows thus constitute a challenging test case for LES. The effects of nonlinear models in these test cases will be studied further in the future.

Furthermore, we searched for a robust definition of the subgrid characteristic length scale that minimizes the dependence of LES results on grid anisotropy. To that end, a new flow-dependent subgrid characteristic length scale was proposed in Eq. (2.12). In this work, this length scale has been successfully tested for simulations of decaying homogeneous isotropic turbulence and plane-channel flow at $\mathrm{Re}_\tau = 395$ using (artificially) refined grids. Comparisons with the classical length scale of Deardorff have shown that the proposed definition is much more robust with respect to mesh anisotropies. In addition, it is very easy to implement. Therefore, the currently proposed length scale has great potential to be used in LES of flows in complex geometries where highly skewed (unstructured) meshes may be present.

As such, we have obtained promising results for the modeling of transport processes in anisotropic flows and for performing LES on anisotropic grids, and we hope to combine these features in future studies.

Acknowledgments

We are grateful to Stefan Hickel for his assistance in setting up numerical simulations of rotating homogeneous isotropic turbulence. The authors also acknowledge use of computational resources from the Certainty cluster awarded by the National Science Foundation to CTR.

REFERENCES

Chauvet, N., Deck, S. & Jacquin, L. 2007 Zonal detached eddy simulation of a controlled propulsive jet. *AIAA J.* **45**, 2458–2473.

Comte-Bellot, G. & Corrsin, S. 1971 Simple Eulerian time correlation of full- and narrow-band velocity signals in grid-generated, isotropic turbulence. *J. Fluid Mech.* **48**, 273–337.

Deardorff, J. 1970 Numerical study of three-dimensional turbulent channel flow at large Reynolds numbers. *J. Fluid Mech.* **41**, 453–480.

Germano, M., Piomelli, U., Moin, P. & Cabot, W. 1991 A dynamic subgrid-scale eddy viscosity model. *Phys. Fluids A* **3**, 1760–1765.

Grundestam, O., Wallin, S. & Johansson, A. 2008 Direct numerical simulations of rotating turbulent channel flow. *J. Fluid Mech.* **598**, 177–199.

Lund, T. & Novikov, E. 1992 Parameterization of subgrid-scale stress by the velocity gradient tensor. *Annual Research Briefs,* Center for Turbulence Research, Stanford University, pp. 27–43.

Marstorp, L., Brethouwer, G., Grundestam, O. & Johansson, A. 2009 Explicit algebraic subgrid stress models with application to rotating channel flow. *J. Fluid Mech.* **639**, 403–432.

Montecchia, M., Rasam, A., Brethouwer, G. & Johansson, A. 2015 Large-eddy simulation of turbulent channel flow using the explicit algebraic subgrid-scale model. In *15th European Turbulence Conference, Delft, The Netherlands, August 25-28, 2015*.

Moser, R. D., Kim, J. & Mansour, N. N. 1999 Direct numerical simulation of turbulent channel flow up to $\mathrm{Re}_\tau = 590$. *Phys. Fluids* **11**, 943–945.

Pope, S. 1975 A more general effective-viscosity hypothesis. *J. Fluid Mech.* **72**, 331–340.

Rasam, A., Brethouwer, G., Schlatter, P., Li, Q. & Johansson, A. 2011 Effects of modelling, resolution and anisotropy of subgrid-scales on large eddy simulations of channel flow. *J. Turbul.* **12**, N10.

Rozema, W., Bae, H., Moin, P. & Verstappen, R. 2015 Minimum-dissipation models for large-eddy simulation. *Phys. Fluids* **27**, 085107.

Sagaut, P. 2006 *Large Eddy Simulation for Incompressible Flows*, 3rd edn. Springer-Verlag Berlin Heidelberg.

Scotti, A., Meneveau, C. & Lilly, D. K. 1993 Generalized Smagorinsky model for anisotropic grids. *Phys. Fluids* **5**, 2306–2308.

Spalart, P. R., Jou, W. H., Strelets, M. & Allmaras, S. R. 1997 Comments on the feasibility of LES for wings, and on a hybrid RANS/LES approach. In *Advances in DES/LES* (ed. C. Liu & Z. Liu). Greyden Press, Columbus, OH.

Trias, F. X., Folch, D., Gorobets, A. & Oliva, A. 2015 Building proper invariants for eddy-viscosity subgrid-scale models. *Phys. Fluids* **27**, 065103.

Trias, F. X., Gorobets, A. & Oliva, A. 2013 A simple approach to discretize the viscous term with spatially varying (eddy-)viscosity. *J. Comput. Phys.* **253**, 405–417.

Verstappen, R. W. C. P. & Veldman, A. E. P. 2003 Symmetry-preserving discretization of turbulent flow. *J. Comput. Phys.* **187**, 343–368.

Winckelmans, G., Jeanmart, H. & Carati, D. 2002 On the comparison of turbulence intensities from large-eddy simulation with those from experiment or direct numerical simulation. *Phys. Fluids* **14**, 1809–1811.